

## Influence of reactant vibrational excitation on stereodynamics of $C + NO \rightarrow CN + O$ Reaction

Qiang Wei\*

*School of Opoelectronic Information, Chongqing University of Technology,  
Chongqing 400050, China*

Received 16 February 2016; Accepted (in revised version) 21 April 2016

Published Online 25 May 2016

---

**Abstract.** Stereodynamics of the title reaction at different reagent vibrational states ( $v=0-2$ ) are obtained using the quasiclassical trajectory method at collision energy of 0.06 eV on an accurate  ${}^4A''$  potential energy surface. The vector properties including angular momentum  $P(\theta_r)$  and  $P(\phi_r)$  distributions as well as polarization-dependent differential cross sections (PDDCS) of the product CN are presented. Furthermore, the influence of vibrational excitation on the product vector properties has also been studied in present work.

**PACS:** 34.35.+a, 34.50.-s

**Key words:** stereodynamics; vibrational excitation; quasiclassical trajectory.

---

### 1 Introduction

The CNO reaction systems are relevant to astrochemistry under the cold conditions and are especially important for understanding the processes of NO reburning at high combustion temperatures. [1-2] Due to their eminence in gas phase chemistry, the CNO reaction systems have attracted much theoretical and experimental attention. A large number of experiments [3-11] have been carried out to measure the product energy partitioning and rovibrational distributions of CN, the reaction cross section as well as the rate coefficients at room temperature and low-temperature for the reaction.

From the theoretical viewpoint, the CNO potential energy surfaces have been builded and dynamical calculations have been carried out in recent years. The first *ab initio* study of the CNO PES was constructed by Persson *et al.* [12] The geometries and vibrational frequencies for the stationary points were determined for both  ${}^2A'$  and  ${}^2A''$  PESs. [13] Based on these surfaces, the followed work focused on the classical dynamics studies and rovibrational spectral of the linear triatomic molecules CNO. [14] However, the above  ${}^2A'$  and

---

\*Corresponding author. *Email address:* qiangwei@cqut.edu.cn (Q. Wei)

$^2A''$  potential energy surface was much too attractive for non-linear approaches of C to NO as pointed by Nyman and coworkers, which result in the overestimate the rate coefficient at room temperatures and were not good enough to describe the long-range interaction. To get more accurate rate coefficient and better simulate the results of the crossed molecular beam experiment, Nyman and coworkers improved and reconstructed the  $^2A'$  and  $^2A''$  PESs. [15-16] Thermal rate coefficients for formation of CN+O and CO+N in the temperature range from 200 K to 4500 K have been obtained using quasiclassical trajectory calculations and agreed excellent with experiment based on the new surface. [17-18] Very recently, Nyman and coworkers built a new  $^4A''$  PES for this reaction to explain the direct formation of ground state N atom in the crossed molecular beam experiment. [19] The inclusion of the  $^4A''$  surface in the QCT calculations gave more excellent agreement with experiments. In 2012, the thermal rate constants for reaction have been recalculated in  $^2A'$ ,  $^2A''$  and  $^4A''$  electronic states by using the adiabatic capture centrifugal sudden approximation and QCT method [20].

For fully understanding the dynamics of the title reaction, it is important to study not only its scalar properties as mentioned above, but also to study its vector properties such as relative velocities of reagent and product and the product rotational angular momentum etc. The vector properties of chemical reaction can provide the valuable information about chemical reaction stereodynamics. Ma and coworkers have carried out stereodynamics study for C+NO reaction at 0.06 eV based on the  $^2A'$  and  $^2A''$  PESs. [21-22] Very recently, we have carried out the QCT calculation to study the rotational excitation effect on the stereodynamics of this reaction on the new  $^4A''$  PES for comparison with the work of Ma and coworkers. [23-24] In the present paper, we applied the QCT method to study the vibrational excitation influence on the stereodynamics of the title reaction on  $^4A''$  PES.

## 2 Theory

The present calculations were performed by applying a standard QCT-stereodynamics procedure which has been successfully used to study a great deal of collision reactions. The center-of-mass (c.m.) frame is utilized in our calculations. The z-axis is parallel to the reagent relative velocity vector  $k$ , while the xz-plane (also called the scattering plane) contains  $k$  and  $k'$  with  $k'$  on the  $x \geq 0$  half plane. The y-axis is perpendicular to the scattering plane,  $\theta_r$  is the angle between  $k$  and  $j'$ ,  $\phi_r$  is the dihedral angle between the scattering plane and the plane containing  $k$  and  $j'$ ,  $\theta_t$  is the angle between  $k$  and  $k'$ . In the c.m. frame, the product rotational polarization can be depicted through angular distributions  $P(\theta_r)$ ,  $P(\phi_r)$  and polarization-dependent generalized differential cross sections (PDDCSs). The product rotational polarization for the title reactions is investigated, using the stereo-QCT procedure which was developed by Han *et al.* [25-27]. Each reaction runs 100 000 trajectories and the integration step size is set as 0.1 fs to guarantee the conservation of total angular momentum and total energy. The calculations of the product

rotational polarization with the initial rotational quantum number  $j=0$  and initial vibrational quantum number  $v=0$ . The collision energy is 10kcal/mol and the initial collision length is 15Å for each reaction.

The general theory of the product rotational polarization is standard, and here we only provide a simple description relevant to the present work. The reference frame used in this work is the center-of-mass (CM) frame, which is shown in Fig. 1. The reagent relative velocity vector  $k$  is parallel to the  $z$  axis and the  $x$ - $z$  plane is the scattering plane containing the initial and final relative velocity vectors,  $k$  and  $k'$ . The angle  $\theta_t$  is the so-called scattering angle between the reagent relative velocity and the product relative velocity. The angles  $\theta_r$  and  $\phi_r$  are the polar and azimuthal angles of the final rotational angular momentum  $j'$ .

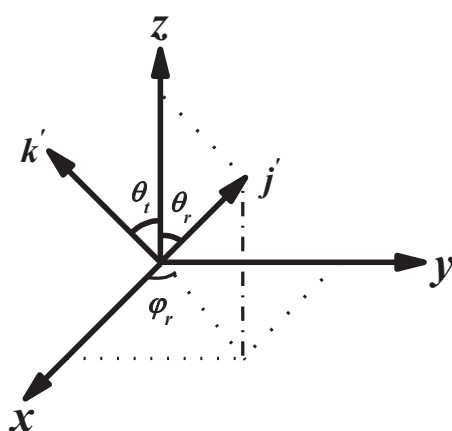


Figure 1: The center-of-mass coordinate system used to describe the  $k$ ,  $k'$  and  $j'$  correlations.

The distribution function  $P(\theta_r)$  and the dihedral angle distribution function  $P(\phi_r)$  described the  $k$ - $j'$  and  $k$ - $k'$ - $j'$  correlations, respectively. The function  $P(\theta_r)$  can be expanded in a series of Legendre polynomials as

$$P(\theta_r) = \frac{1}{2} \sum_k (2k+1) a_0^{(k)} P_k(\cos\theta_r). \quad (1)$$

Where

$$a_0^{(k)} = \int_0^\pi P(\theta_r) P_k(\cos\theta_r) \sin\theta_r d\theta_r = \langle P_k(\cos\theta_r) \rangle. \quad (2)$$

The expanding coefficients  $a_0^{(k)}$  are called the orientation ( $k$  is odd) or alignment ( $k$  is even) parameters. The dihedral angle distribution function  $P(\phi_r)$  can be expanded in a series of Fourier series as

$$P(\phi_r) = \frac{1}{2\pi} \left( 1 + \sum_{\text{even}, n \geq 2} a_n \cos n\phi_r \right) + \sum_{\text{odd}, n \geq 1} b_n (\sin n\phi_r). \quad (3)$$

Where

$$a_n = 2\langle \cos n\phi_r \rangle \quad (4)$$

$$b_n = 2\langle \sin n\phi_r \rangle. \quad (5)$$

In this calculation,  $P(\theta_r)$  and  $P(\phi_r)$  are expanded up to  $k=18$ ,  $n=24$ , respectively, which thereby showing good convergence.

The fully correlated CM angular distribution is written as the sum:

$$P(\omega_t, \omega_r) = \sum_{kq} \frac{[k]}{4\pi} \frac{1}{\sigma} \frac{d\sigma_{kq}}{d\omega_t} C_{kq}(\theta_t, \theta_r) \quad (6)$$

where,  $[k]=2k+1$ ,  $C_{kq}(\theta_t, \theta_r) = \sqrt{4\pi/(2k+1)} Y_{kq}(\theta_t, \theta_r)$  is modified spherical harmonics,  $(1/\sigma)(d\sigma_{kq}/d\omega_t)$  is a generalized PDDCSs and yields

$$\frac{1}{\sigma} \frac{d\sigma_{k0}}{d\omega_t} = 0, \quad k \text{ is odd} \quad (7)$$

$$\frac{1}{\sigma} \frac{d\sigma_{kq\pm}}{d\omega_t} = \frac{1}{\sigma} \frac{d\sigma_{kq}}{d\omega_t} + \frac{1}{\sigma} \frac{d\sigma_{k-q}}{d\omega_t} = 0, \quad k \text{ is even and } q \text{ is odd or } k \text{ is odd and } q \text{ is even} \quad (8)$$

$$\frac{1}{\sigma} \frac{d\sigma_{kq-}}{d\omega_t} = \frac{1}{\sigma} \frac{d\sigma_{kq}}{d\omega_t} - \frac{1}{\sigma} \frac{d\sigma_{k-q}}{d\omega_t} = 0, \quad k \text{ is even and } q \text{ is even or } k \text{ is odd and } q \text{ is odd.} \quad (9)$$

The PDDCS can write as

$$\frac{1}{\sigma} \frac{d\sigma_{kq\pm}}{d\omega_t} = \sum_{k_1} \frac{k_1}{4\pi} S_{kq\pm}^{k_1} C_{k_1q}(\theta_t, 0). \quad (10)$$

Where  $S_{kq\pm}^{k_1}$  is an expected value and write as

$$S_{kq\pm}^{k_1} = \langle C_{k_1q}(\theta_t, 0) C_{kq}(\theta_r, 0) [(-1)^q e^{iq\zeta\phi_r} \pm e^{-iq\phi_r}] \rangle \quad (11)$$

the angular brackets represent average over the all angles.

In the present work, we calculated the  $k=0$  and  $k=2$ ,  $(2\pi/\sigma)(d\sigma_{00}/d\omega_t)$ ,  $(2\pi/\sigma)(d\sigma_{20}/d\omega_t)$ ,  $(2\pi/\sigma)(d\sigma_{22+}/d\omega_t)$ , and  $(2\pi/\sigma)(d\sigma_{21-}/d\omega_t)$  named PDDCS<sub>00</sub>, PDDCS<sub>20</sub>, PDDCS<sub>22+</sub> and PDDCS<sub>21-</sub> are calculated by using the computational code developed by Han and coworkers.

We choose the trajectory initiated with the NO molecule in the  $v=0-2$  and  $j=0$  levels. The initial collision length is 15Å and the collision energy is chosen at 0.06 eV for comparison with previous work. For each reaction, a batch of 100 000 trajectories is run and the integration step is chosen be 0.1 fs.

### 3 Result and discussion

The calculated  $P(\theta_r)$  distributions for CN+O channel of all vibrational states at 0.06 eV ( $\sim 1.5$  kcal/mol) of this reaction are plotted in Fig. 2. As mentioned above, the distribution of the product describes the  $k-j'$  correlation. It is clearly seen from Fig. 2, at all

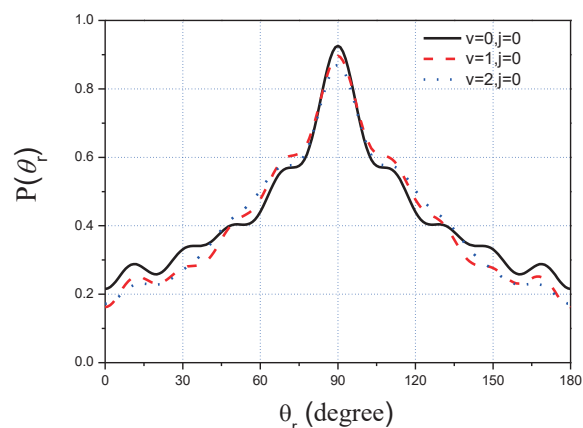


Figure 2: The distributions of  $P(\theta_r)$  at collision energies of 0.06 eV for vibration quantum number  $v=0-2$ .

vibrational states, the distributions peak at angles which is close to  $90^\circ$ , and is symmetric with respect to  $90^\circ$ . This shows that the product rotational angular momentum vector is strongly aligned along the direction at the right angle to the relative velocity direction. The alignment becomes weaker and weaker with the vibrational excitation because the peaks of  $P(\theta_r)$  become little lower and broader. In our previous paper, it is found that the rotational excitation also decreased the degree of alignment for CN product. Furthermore the similar situation was also found for CO product.

The dihedral angle distributions  $P(\phi_r)$  of the  $\text{C} + \text{NO} \rightarrow \text{CO} + \text{N}$  reaction at the collision energy of 0.06 eV on the  $^4\text{A}''$  PES for three reagent vibrational states ( $v=0-2$ ) are presented in Fig. 3. As we know, the  $\phi_r$  defines the dihedral angle between the planes consisting of  $k-k'$  and  $k-j'$ , the dihedral angle distributions  $P(\phi_r)$  describes the  $k-k'-j'$  correlation and can provide stereodynamical information on both product alignment and

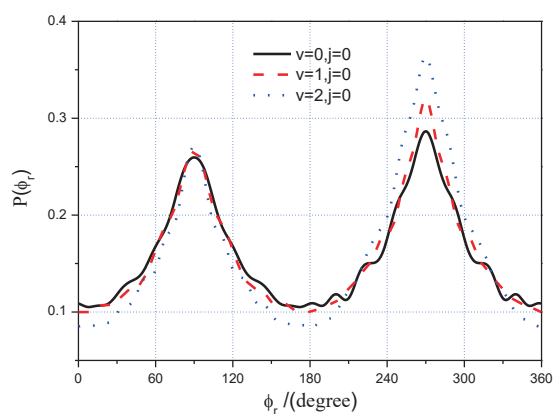


Figure 3: The distributions of  $P(\phi_r)$  at collision energies of 0.06 eV for vibration quantum number  $v=0-2$ .

product orientation. As can be seen from Fig. 3, These peaks appear at around  $= 90^\circ$  and  $270^\circ$ , which indicates that the rotational angular momentum vector of the products are mainly aligned along y-axis of the CM frame. In addition, we can also see that the distributions are tend to be asymmetric with respect to the  $k-k'$  scattering plane (or about  $= 180^\circ$ ), because peaks at  $270^\circ$  are larger than those at  $90^\circ$  for  $v=0-2$ . That is to say there exists some preference for the product molecules rotating clockwise in the plane parallel to the scattering plane (see from the right side of the plane). It is should be mentioned that the peaks at  $270^\circ$  show somewhat increase with the vibrational excitation but almost no change at  $90^\circ$ , implying that both alignment and orientation of the product CN become stronger at higher vibrational level. However, unlike the vibration excitation, it was found that the product orientation become weaker with rotation excitation in previous research.

Four PDDCSs of the CN for the title reaction calculated at the three different vibrational states are presented in Fig. 4. The PDDCS00, which is simply proportional to the differential cross-section (DCS), only describes the correlation or the scattering direction of the product. From Fig. 4(a), we can see that the distributions are clearly dominated

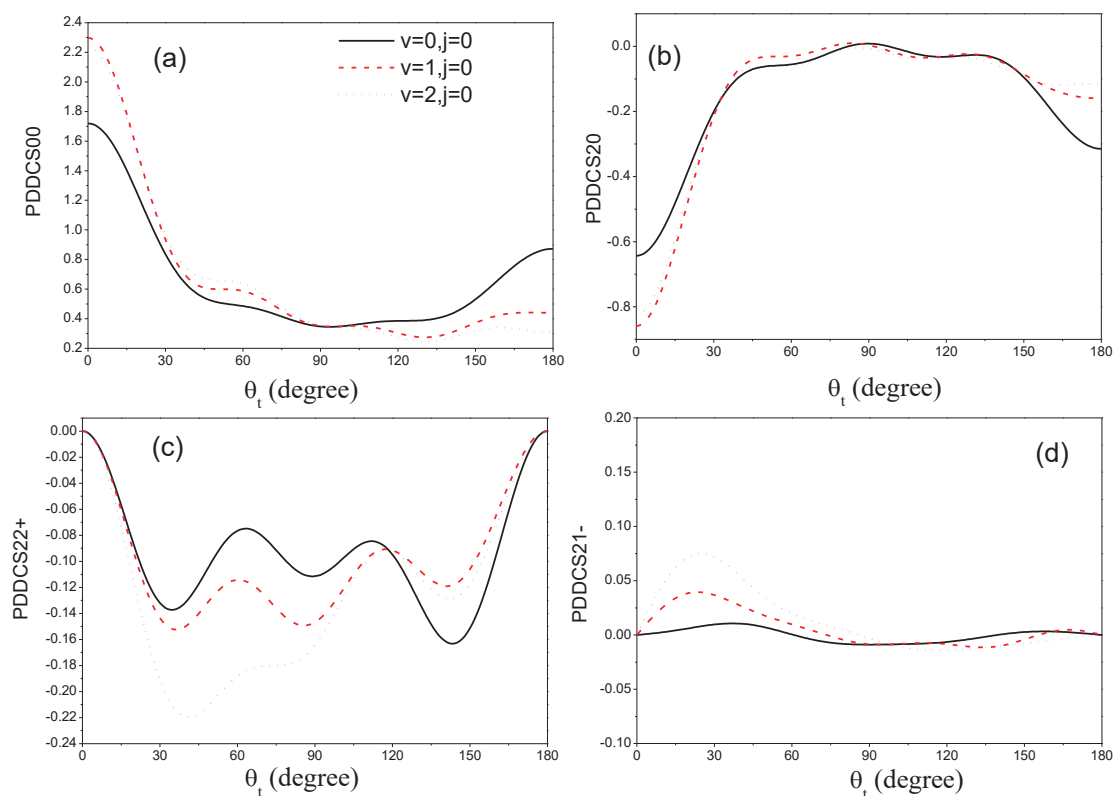


Figure 4: Four PDDCSs (PDDCS00, PDDCS20, PDDCS22+, PDDCS21-) at collision energies of 0.06 eV for vibration quantum number  $v=0-2$ .

by a forward peak and a smaller backward peak at three vibrational states, respectively. In addition, the forward scattering increases with the vibrational excitation. The distribution of PDDCS20 contains the information that the alignment of  $j'$  with respect to  $k$  as a function of scattering angle. From Fig. 4(b), one can see that the values of PDDCS20 are all negative for backward and forward scattered products, and are approximately zero for sideway scattered products. Overall, the results for three different vibrational states show the same general trends. It is noted that the  $j'$  is strongly aligned and polarized with the scattering angle at three vibrational states, where the largest peak is at about  $180^\circ$ . The value of PDDCS22+ is positive or negative indicates the preference of  $j'$  alignment along the x axis or y axis, respectively. As can be seen from Fig. 4(c), PDDCS22+ exhibits a strong dependence on the scattering angle, and is clearly a noticeable preference for an alignment of  $j'$  along the y axis as opposed to the x axis. According to the value of PDDCS21-, shown in Fig. 6(d), one could clearly distinguish whether the product is aligned along the direction of the vector x-z or x+z. The positive value PDDCS21- reveals the product alignment along x-z axis. Conversely, the alignment is along x+z axis and the value is close to zero, there are no obvious alignment directions. Generally, the larger absolute value suggests the stronger alignment along the relevant axis. As can be seen from Fig. 4(d), the value of PDDCS21- are almost zero at all scattering angle and oscillated around zero. This reveals that the rotational angular momentum distributions are almost isotropic at the scattering angle. In addition, the rotational momentum distributions are very weakly influenced by vibrational excitation.

## 4 Conclusion

In this paper, the  $P(\theta_r)$ ,  $P(\phi_r)$  as well as four normalized PDDCSs were calculated at different vibration states by means of QCT method. The results indicate that rotational angular momentum vector  $j'$  of product CN was preferentially aligned perpendicular to  $k$  and was also oriented with respect to the  $k$ - $k'$  plane at all vibration states. The intensities of  $P(\theta_r)$  decreased with vibrational excitation, but the intensities of  $P(\phi_r)$  have opposite trend. The PDDCS<sub>00</sub> showed that the product CN were preferentially forward scattering and began to increase with vibrational excitation. The vibrational excitation has little effect on the behavior of PDDCS22+ but almost no effect on PDDCS20 and PDDCS21-.

**Acknowledgments.** This work is supported by the Natural Science Foundation of China (No. 11204392 and No. 11047125) and Scientific and Technological Research Program of Chongqing Municipal Education Commission (Grant No. KJ1400920). The author also acknowledges Professor Keli Han for providing the QCT code of stereodynamics.

## References

- [1] P. Glarborg, M. U. Alzueta, K. D. Johansen and J. A. Miller, *Combust. Flame*. 115 (1998) 1.
- [2] G. I. Boger and A. Sternberg, *Astrophys. J.* 632 (2005) 302.

- [3] W. Braun, A. M. Bass, D. D. Davis and J. D. Simmons, Proc. R. Soc. A. 312 (1969) 417.
- [4] H. F. Krause, Chem. Phys. Lett. 78 (1981) 78.
- [5] A. Bergeat, T. Calvo, G. Dorthe and J. C. Loison, Chem. Phys. Lett. 308 (1999) 7.
- [6] D. Husain and L. J. Kirsch, Chem. Phys. Lett. 8 (1971) 543.
- [7] P. Halvick, J. C. Rayez and E. M. Evleth, J. Chem. Phys. 81 (1984) 728.
- [8] P. Halvick and J. C. Rayez, Chem. Phys. 131 (1989) 375.
- [9] A. J. Dean, R. K. Hanson and C. T. Bowman, J. Phys. Chem. 95 (1991) 3180.
- [10] C. Naulin, M. Costes and G. Dorthe, Chem. Phys. 153 (1991) 519.
- [11] M. Costes, C. Naulin, N. Ghanem and G. Dorthe, J. Chem. Soc. Faraday Trans. 89 (1993) 1501.
- [12] B. J. Persson, B. O. Roos and M. Simonson, Chem. Phys. Lett. 234 (1995) 382.
- [13] B. J. Persson, B. O. Roos and S. Carter, Mol. Phys. 84 (1995) 619.
- [14] A. J. Dean, R. K. Hanson and C. T. Bowman, J. Phys. Chem. 95(1991) 180.
- [15] S. Andersson, N. Markovic and G. Nyman, 259 Chem. Phys. (2000) 99.
- [16] S. Andersson, N. Markovic and G. Nyman, Phys. Chem. Chem. Phys. 2 (2000) 613.
- [17] E. Abrahamsson, S. Andersson, G. Nyman and N. Markovic, 324 Chem. Phys (2006) 507.
- [18] S. Andersson, N. Markovic and G. Nyman, J. Phys. Chem. A107 (2003) 5439.
- [19] E. Abrahamsson, S. Andersson, G. Nyman and N. Markovic, Phys. Chem. Chem. Phys. 10 (2008) 4400.
- [20] T. J. Frankcombe and S. Andersson, J. Phys. Chem A 116 (2012) 4705.
- [21] J. J. Ma and S. L. Cong, J. At. Mol. Phys 26 (2009) 1081.
- [22] J. J. Ma, Y. Zou and H. T. Liu, Chin. Phys. B 22 (2013) 063402.
- [23] Q. Wei, CHIN. PHYS. LETT. 32 (2015) 013101.
- [24] Q. Wei, Acta Phys. Sin. 64 (2015) 173401.
- [25] K. L. Han, G. Z. He and N. Q. Lou, Chin J. Chem. Phys. 2 (1989) 323.
- [26] K. L. Han, G. Z. He and N. Q. Lou, Chin Phys. Lett. 4 (1993) 517.
- [27] R. J. Li, K. L. Han, F. E. Li, G. Z. He and N. Q. Lou, Chem Phys Lett. 220 (1994) 281.